2006-01-2326

# Posture Prediction and Force/Torque Analysis for Human Hands

**Jingzhou Yang*, Esteban Pena Pitarch, Joo Kim, and Karim Abdel-Malek**
Virtual Soldier Research (VSR) Program, Center for Computer-Aided Design, The University of Iowa



## ABSTRACT

Human hands are the bridge between humans and the objects to be manipulated or grasped both in the real and virtual world. Hands are used to grasp or manipulate objects and one of the most important functionalities is to position the fingers, i.e., given the position of the fingertip and to determine the joint angles. Last year we presented a 25-degree of freedom (DOF) hand model that has palm arch functionality. In this paper we preset an optimization-based inverse kinematics approach to position this 25 DOF hand locally with respect to the wrist instead of the traditional Moore-Penrose pseudo-inverse and experiment methods. The hypothesis is that human performance measures govern the configuration and motion of the hand. We also propose contact force and joint torque prediction. The exposition addresses (1) the determination whether a point is reachable (i.e., is it within the reach envelope), (2) the prediction of a finger posture for a given target point, (3) given the finger contact force analyzing the joint torque, and (4) given joint torque analyzing finger contact force. We illustrate the methodology through examples.

Keywords: Virtual humans, human performance measures, inverse kinematics, hand posture.

## INTRODUCTION

Apart from the advantages that the use of a man model technique might bring in terms of cost and time delay, for such a model to be truly useful, it must be closely integrated with a detailed hand model to be positioned globally or locally. To explain the meaning of posture prediction, consider a given point in space (e.g., a target), where it is required to determine the joint angles that configure the hand that allow a specified point on each finger to touch its target point. There have been two schools of thought regarding hand posture prediction. The first, perhaps the more traditional, uses empirical data, collected from performing thousands of experiments by human subjects, or simulation using 3D computer-aided man-modeling software [see for instance; Lee and Zhang (2005)], which were statistically analyzed to form a predictive model of posture; e.g. regression models. The experimental school of thought is referred to as the empirical-statistical modeling method (Beck and Chaffin 1992; Zhang and Chaffin 1996; Das and Behara 1998; and Faraway, et al. 1999).

The second school of thought uses mathematically models based on geometry or analytical expressions to predict the inverse kinematics. In the field of kinematics, this problem is called inverse kinematics. We shall call this school of thought the mathematical-based approach (Kee et al. 1994; Jung et al. 1995a; Jung and Kee 1996; Jung and Choe 1996; Kee and Kim 1997; and Wang 1999). While some researchers that belong to the first school of posture prediction (in particular Beck and Chaffin 1992) cautioned that inverse kinematics is not necessarily correct for prediction of posture because of its theoretical foundation. Others (Faraway, et al. 1999) have also argued that postures that are modeled using angles between body segments, rather than joint coordinates, may violate task constraints. The concept of cost function for posture prediction is not new. Many researchers have addressed this problem but we only cite references in this paper (Jung, et al. 1992, 1994, 1995a,b; Jung and Choe 1996; Jung and Kee 1996; Dysart and Woldstad 1996; Wang 1999; Kee and Kim 1997).

The purpose of this work is to develop an optimization-based approach locally to position the 25 DOF hand model developed in the VSR group at the University of Iowa (Pena Pitarch et al 2005), analyze the joint torques given the finger contact forces, and vise versa. The cost function is the joint displacement that was used in Jung et al. (1995a).

## HAND MODEL

Fig. 1 and 2 show the 25 DOF left and right hand models, respectively. All of joints in the hand are revolute and if we use a generalized coordinate $q_i$ that represents one degree of freedom, then the generalized coordinate vector can be represented by $\mathbf{q} = \left[ (\mathbf{q}^1)^T \quad \cdots \quad (\mathbf{q}^{10})^T \right]^T = [q_1, ..., q_{50}]^T$.

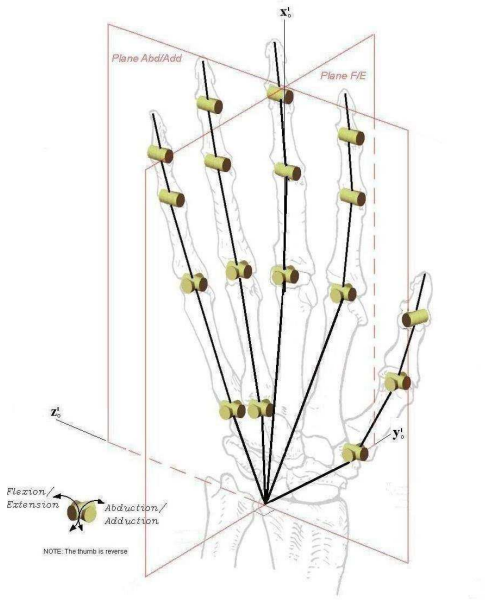


Fig. 1 Dorsal view left hand model

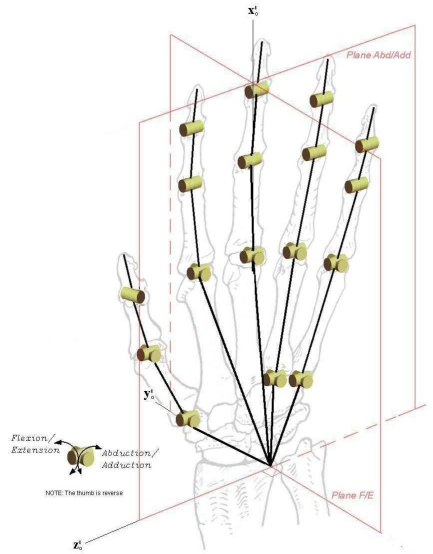


Fig. 2 Dorsal view right hand model

This hand model has the capability for anthropometric variability shown in Figs. 3 and 4 which are scalable link length (Buchcholtz *et al* 1993) and joint limit, respectively.

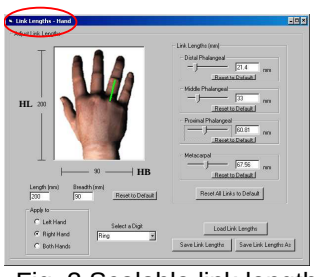

Fig. 3 Scalable link length

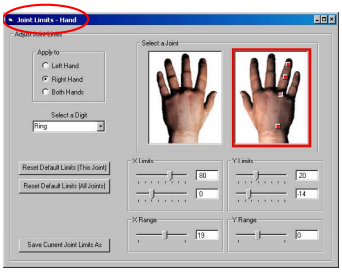

Fig. 4 Scalable joint limit

## METHODS

In this paper, we explore the use of optimization-based approach to determine the hand posture. We will address the following problems:
(1) Given a target point in space, is this point reachable?
(2) Given a target point in space, what are the joint angles that would configure the hand such that an anatomical landmark on the finger will reach the target point?

### REACH ENVELOPE

The D-H **(**Denavit and Hartenberg 1955**)** representation provides a systematic method for describing the relationship between adjacent links. A position vector of an anatomical landmark on the end-effector of a human hand articulated model can be written in terms of joint coordinates as

$$\mathbf{x} = \mathbf{\Phi}(\mathbf{q}^i) \tag{1}$$

where $\mathbf{q}^i \in \mathbf{R}^n$ is the vector of *n*-generalized coordinates. In order to extend the formulation to include ranges of motion in the form of inequality constraints such as $q_i^{\min} \le q_i \le q_i^{\max}$ (e.g., the range of motion of the elbow is approximately $0^o \le q \le 150^o$), a transformation is introduced as

$$q_i = a_i + b_i \sin \lambda_i \tag{2}$$

where $a_i = \left(q_i^{\max} + q_i^{\min}\right)/2$ and $b_i = \left(q_i^{\max} - q_i^{\min}\right)/2$ are the mid point and half range of the inequality constraint and $\lambda$ is a slack variable (i.e., we have converted the inequality to an equality). To study the boundary of this function, we use the implicit function theorem to determine the reach envelope (Yang et al. 2005). Indeed, if we differentiate Eq. (4) with respect to time to obtain the velocity, the right hand side will comprise two matrices and the joint velocity vector as

$$\dot{\mathbf{x}} = \mathbf{\Phi}_{\mathbf{q}^i} \mathbf{q}_{\boldsymbol{\lambda}}^i \dot{\boldsymbol{\lambda}} \tag{3}$$

where $\mathbf{q}_{\boldsymbol{\lambda}}^i = \partial q_i / \partial \lambda_j$ is a diagonal matrix, $\dot{\boldsymbol{\lambda}} = d\boldsymbol{\lambda}/dt$ is the vector of joint velocities, and $\mathbf{\Phi}_{\mathbf{q}^i}$ is the Jacobian defined by

$$\mathbf{\Phi}_{\mathbf{q}^i} = \left[\partial \Phi_i / \partial q_j\right] \tag{4}$$

It is then possible to delineate singular surfaces that are on the boundary of the reacheable workspace, i.e., the reach envelope. This is accomplished by studying the rank deficiency of the Jacobian. Define the subvector of $\mathbf{q}^i$ as a set of constant generalized coordinates $\mathbf{p}_i \in \mathbf{R}^m$ where $m \le n-1$, and $\mathbf{q}^i = \mathbf{u} \cup \mathbf{p}_i$. Singular sets $\mathbf{p}_i$ of the manipulator can be obtained from studying the dimension of the null space of $\mathbf{\Phi}_{\mathbf{q}^i}^T(\mathbf{q}^i)$, defined by Yang et al. (2004) as the set

$$\mathbf{S} = \left\{\mathbf{p}_i \in \mathbf{R}^m ; \dim\left[Null(\mathbf{\Phi}_{\mathbf{q}^i}^T(\mathbf{q}^i))\right] \ge 1, \mathbf{q}^i = \begin{bmatrix}\mathbf{u} & \mathbf{p}_i\end{bmatrix} \text{ for some constant } \mathbf{p}_i\right\} \tag{5}$$

where $\mathbf{u} \in \mathbf{R}^{n-m}$ is the vector of generalized coordinates that are not in $\mathbf{p}_i$. On a singular surface, the term $\mathbf{\Phi}_{\mathbf{q}^i} \mathbf{q}_{\boldsymbol{\lambda}}^i \Big|_{\mathbf{q}_o^i, \boldsymbol{\lambda}_o}$ is rank-deficient. Therefore, a boundary is identified when the rows of $\mathbf{\Phi}_{\mathbf{q}^i} \mathbf{q}_{\mathbf{s}}^i$ are dependent. As a

result, the sets of singular values $\mathbf{p}_i$ are identified and substituted into $\Phi(\mathbf{q}^i)$ to yield singular surfaces on the boundary of the reach envelope, which we will denote by $\psi(\mathbf{u})$.

Because the above formulation yields a complete exact representation of the boundary to the reach envelope in closed form, it is possible to mathematically determine whether a given point (e.g., a button), curve (i.e., a trajectory), or an object (e.g., a lever) is inside the reach envelope. The parametric surface patches on the boundary of the reach envelope are described by a number of $\psi(\mathbf{u})$ as illustrated in Fig. 5. A point is reachable if it exists inside the reach envelope. Therefore, it is now necessary to establish whether a point is inside the reach envelope. For a number of surface patches, a point (e.g., point **p** in Fig. 5) is inside the envelope if the ray cast from that point intersects an odd number of times with the surface patches. If intersects an even number of times, it is outside (i.e., not reachable).

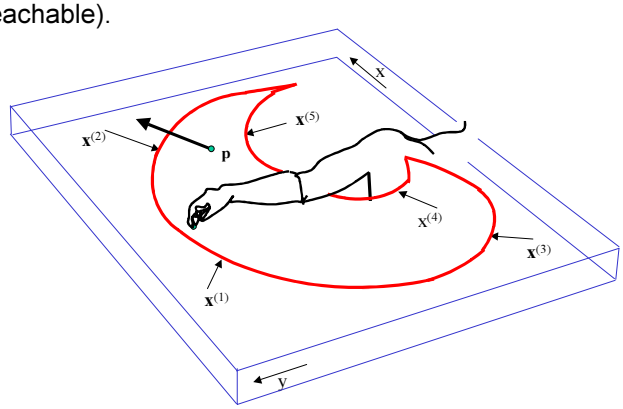

Fig. 5 Determining whether a point is reachable

## OPTIMIZATION APPROACH

The optimization problem for inverse kinematic of the hand is defined as follow:

Find: $\mathbf{q}^i \in R^{n_i}$ (6)

to minimize: *Joint displacement*

subject to: $distance = \left\| \mathbf{x}\left(\mathbf{q}^i\right)^{end\text{-}effector} - \mathbf{x}^{target\ point} \right\| \le \varepsilon$

$q_i^L \le q_i \le q_i^U;\ i = 1, 2, \ldots, n_i$

where $\varepsilon$ is a small number that approximates zero. All optimization problems are solved using the software SNOPT (Gill *et al*, 2002).

It is evident that the motion subtended by the human hand to reach a specific target is directly dependent upon the hand's initial posture (i.e., initial conditions). A person will usually reach towards a target using the least motion of the joints possible. A person will also usually avoid exerting unnecessary energy against gravity. Therefore, we propose driving functions on the motion characterized by minimizing the displacement from the initial posture and minimizing the potential energy exerted towards reaching the target, subject to the kinematic constraints discussed above and each joint's range of motion. Such cost functions can be developed for dexterity, stress, potential and kinetic energy, and force. However, in this preliminary study, we use joint placement function only. Consider a simple cost function that measures the level of joint displacement from the most neutral position of a given joint. Let $q_i^N$ be the neutral position of a joint. Then the displacement from the neutral position is given by $q_i - q_i^N$. Because the joint displacement is usually felt higher in some joints versus others, we also introduce a weight function $w_i$ to stress the importance of one joint versus another. The total joint displacement of all joints is then characterized by the function

$$f_d = \sum_{i=1}^{n} w_i \left| q_i - q_i^N \right| \tag{7}$$

## JOINT TORQUE ANALYSIS

Since the hand grasping velocity and acceleration are small, we consider hand grasping as one static problem. Therefore, finger joint torques will be the general static torques.

From the time differentiation of the linear and angular position using the chain rule, we can obtain the linear relationship between the linear/angular velocity vector (in Cartesian space) and the joint velocity vector (in joint space) as follows:

$$\begin{bmatrix} \mathbf{v} \\ \boldsymbol{\omega} \end{bmatrix} = \mathbf{J}\left(\mathbf{q}^i\right)\dot{\mathbf{q}}^i \tag{8}$$

where $\mathbf{v}$ is the translational velocity of the end-effector and $\boldsymbol{\omega}$ is the angular velocity of the end-effector frame. $\mathbf{J}(\mathbf{q}^i)$ is the augmented Jacobian matrix of the kinematic structure defined by

$$\mathbf{J}(\mathbf{q}^i) = \begin{bmatrix} \mathbf{J}_x \\ \mathbf{J}_\omega \end{bmatrix} \tag{9}$$

This also indicates that the virtual displacements have the similar relationship.

$$\begin{bmatrix} \delta\mathbf{x} \\ \delta\boldsymbol{\theta} \end{bmatrix} = \mathbf{J}(\mathbf{q}^i)\delta\mathbf{q}^i \qquad \forall \delta\mathbf{q}^i \tag{10}$$

where $\delta\mathbf{x}$, $\delta\boldsymbol{\theta}$, and $\delta\mathbf{q}^i$ are the virtual displacement vectors of Cartesian linear, Cartesian angular, and joint, respectively.

We begin with the calculation of the torque at each joint. To account for all of the elements that enter into calculating the torque at a given joint, we apply the principle of virtual work to the two force systems. As for the joint torques, its associated virtual work is

$$\delta W_\tau = \boldsymbol{\tau}^T \delta\mathbf{q}^i \tag{11}$$

where $\delta W$ is the virtual work. For the end-effector forces $\mathbf{F} = \begin{bmatrix} \mathbf{f}^T & \mathbf{m}^T \end{bmatrix}^T$, comprised of a force vector $\mathbf{f}$ and a moment vector $\mathbf{m}$, the virtual work performed is

$$\delta W_{\mathbf{F}} = \mathbf{f}^T \delta\mathbf{x} + \mathbf{m}^T \boldsymbol{\omega}\delta t \tag{12}$$

where $\delta\mathbf{x}$ is the linear virtual displacement and $\boldsymbol{\omega}\delta t$ is the angular virtual displacement of the end-effector, respectively. Because the difference between the virtual work of the joint torques and the virtual work of the end-effector forces shall be null for all joint virtual displacements, we write

$$\boldsymbol{\tau}^T \delta\mathbf{q}^i = \mathbf{F}^T \mathbf{J}(\mathbf{q}^i)\delta\mathbf{q}^i \qquad \forall \mathbf{q}^i \tag{13}$$

The relationship between the joint torque vector and end-effector force/moment vector is then given by

$$\boldsymbol{\tau} = \mathbf{J}^T \mathbf{F} \tag{14}$$

where the torque vector is $\boldsymbol{\tau} = [\tau_1, \tau_2, ..., \tau_n]^T$ .

Now, we extend this formulation to the case where multiple external loads (both translational and rotational) are applied to any location of any finger/link, not necessarily to the end-effector. Let's assume that a general form of external load $\mathbf{F}_k$ is applied to the point at $\mathbf{k}_{r_k}$ location of finger segment k, where $\mathbf{k}_{r_k}$ location vector is expressed with respect to $k^{th}$ local coordinate frame.

This point of application of external load can be regarded as the end-effector for the corresponding external load. The augmented Jacobian matrix $\mathbf{J}_k$ for this point is derived from the linear relationship between the joint velocity vector and the Cartesian velocity vector:

$$\mathbf{J}_k(\mathbf{q}^i) = \begin{bmatrix} \frac{\partial {}^0\mathbf{T}_1(\mathbf{q}^i)}{\partial q_1} {}^k\mathbf{r}_k & \cdots & \frac{\partial {}^0\mathbf{T}_i(\mathbf{q}^i)}{\partial q_i} {}^k\mathbf{r}_k & \cdots & \frac{\partial {}^0\mathbf{T}_k(\mathbf{q}^i)}{\partial q_k} {}^k\mathbf{r}_k \\ \mathbf{Z}_0(\mathbf{q}^i) & \cdots & \mathbf{Z}_{i-1}(\mathbf{q}^i) & \cdots & \mathbf{Z}_{k-1}(\mathbf{q}^i) \end{bmatrix}_{6\times k} \tag{15}$$

where $\mathbf{Z}_{i-1}, i = 1, ..., k$ is the local z-axis vector of joint *i* expressed in terms of the global coordinate system.

So the joint torque vector due to the external load applied at point $\mathbf{k}_{r_k}$ of link k is

$$\boldsymbol{\tau}_k = \mathbf{J}_k^T \mathbf{F}_k \tag{16}$$

From the principle of superposition, the total joint torques due to several external loads are obtained as a sum of all joint torques:

$$\boldsymbol{\tau} = \sum_k \mathbf{J}_k^T \mathbf{F}_k \tag{17}$$

## FINGER CONTACT FORCE ANALYSIS

Another problem is that given the joint torques we try to find the finger contact forces. Fig. 6 shows the free body diagram of one finger. Based on Eq. (16), if $\mathbf{F}_{n_i}$ is applied on link $n_i$ , the joint torque for joint $n_i$ will be defined by

$$\tau_{n_i} = (J^{n_i}_{n_i-1})^T F_{n_i} \tag{18}$$

For link $n_i - 1$ we have the following equation:

$$\tau_{n_i-1} = (J^{n_i}_{n_i-1})^T F_{n_i} + (J^{n_i-1}_{n_i-2})^T F_{n_i-1} \tag{19}$$

Similarly, for other links and joints we have

$$\vdots$$

$$\tau_1 = (J^{n_i}_{n_i-1})^T F_{n_i} + (J^{n_i-1}_{n_i-2})^T F_{n_i-1} + \cdots + (J^1_0)^T F_1 \tag{20}$$

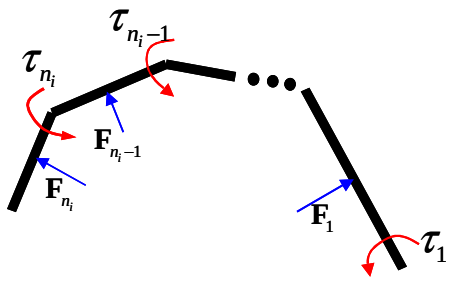


Fig. 6 Joint torque and the contact force diagram

From Eq. (18) we solve the linear equations to obtain $F_{n_i}$ , then plugging $F_{n_i}$ into Eq. (19) and we solve another set of linear equations (19) to obtain $F_{n_i-1}$. Similarly we can derive finger contact forces for other links.

## RESULTS

A person that has the hand with length (HL) 190 mm and hand breadth (HB) 90 mm is considered as the given input (Pena Pitarch et al 2005).

The 4 DOF model for the index finger is shown in Fig. 7 and the DH table in Table 1. By implementing the method presented in the previous section we obtain the reach envelope shown in Fig. 8 and 9.

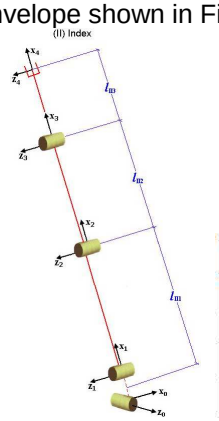


Fig. 7 Index finger model

| | Min. | Max. |
|---|---|---|
| $q_6$ | $\frac{-13}{180}\pi$ | $\frac{7}{30}\pi$ |
| $q_7$ | 0 | $\frac{4}{9}\pi$ |
| $q_8$ | 0 | $\frac{5}{9}\pi$ |
| $q_9$ | $\frac{-\pi}{18}$ | $\frac{\pi}{2}$ |

Table 1 DH table for index

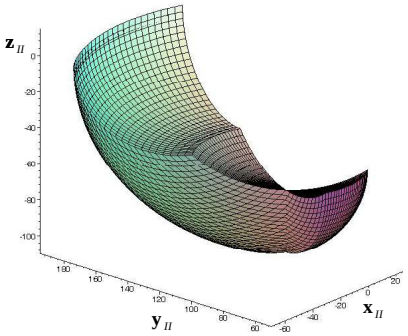


Fig. 8 One view of reach envelope for the index finger

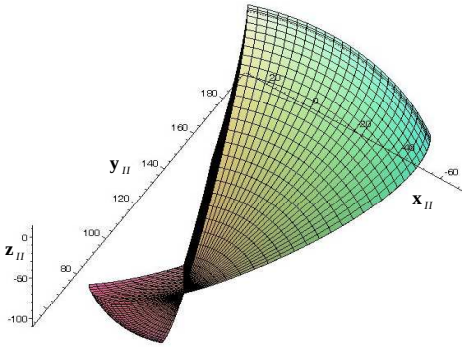


Fig. 9 Another view of reach envelope for the index finger

Posture prediction examples are obtained by implementing the optimization-based approach. Fig. 10 shows the initial configuration the right hand ($q_i = 0, i = 1, \cdots, 25$). Fig. 11 denotes the index finger posture prediction for target point $[12.7839 \quad 7.19009 \quad 0.687351]^T$ and the joint angles are $0^o$, $29^o$, $61.4828^o$ and $27.1936^o$. Fig. 12 shows the experiment visual result for the index finger. Fig. 13 shows the posture prediction for the middle finger. The target point is $[15.9711 \quad 7.74422 \quad -1.62787]^T$ and the predicted joint angles are $0^o$, $30^o$, $30^o$ and $10^o$. Fig. 14 demonstrates the experiment result for the middle finger. Fig. 15 shows the predicted posture for the pinky finger. The target point is $[13.8896 \quad 3.6444 \quad -6.47685]^T$ and the predicted joint angles are $0^o$, $4.6382^o$, $0^o$, $27.1768^o$ and $26.65^o$. Fig. 16 is the experimental result.

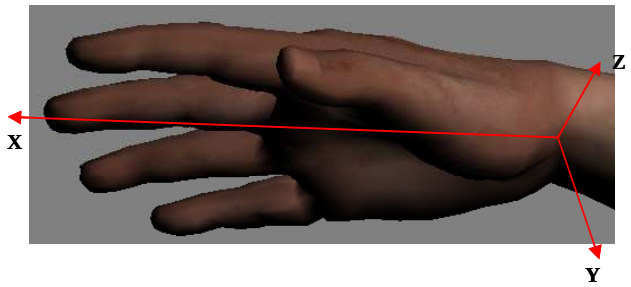


Fig. 10 The initial configuration of the right hand

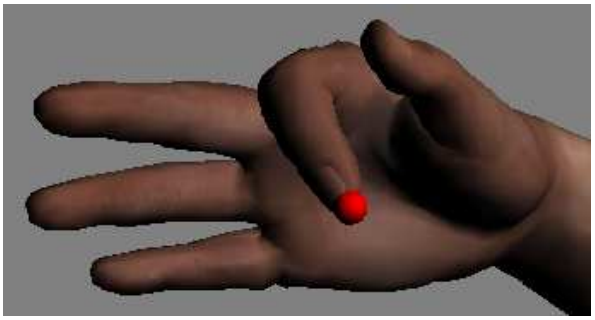

Fig. 11 Posture prediction for the index finger

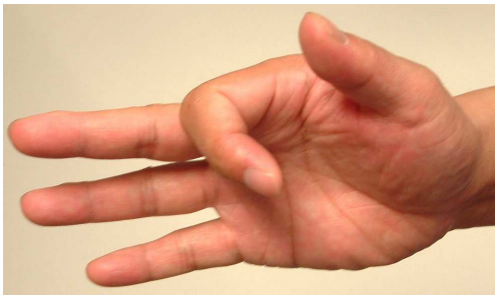

Fig. 12 Experiment posture for the index finger

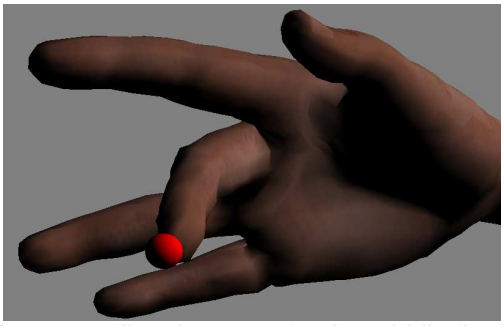

Fig. 13 Predicted posture for the middle finger

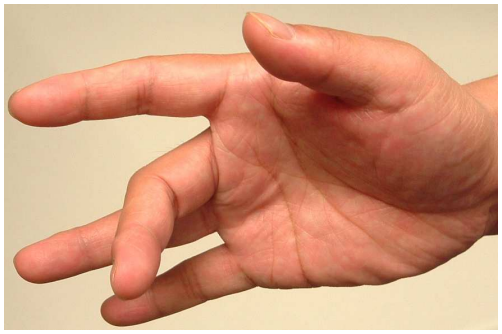

Fig. 14 Experiment posture for the middle finger

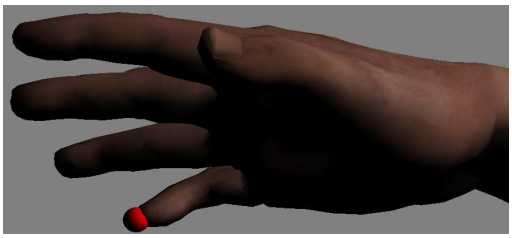

Fig. 15 Predicted posture for the pinky finger

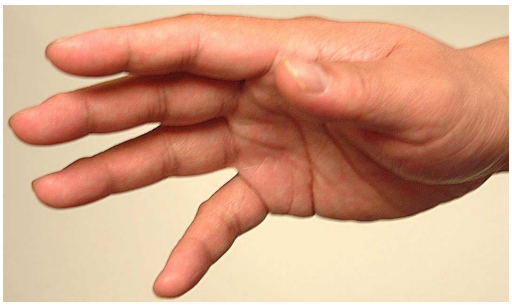

Fig. 16 Experiment posture for the pinky finger

To analyze the joint torque, virtual hand is used to grasp cylinders (Fig. 17) with different radii $\rho$ from 5 mm to 40 mm. For cylinders with radii that are larger than 40 mm, it needs two hands to grasp together. Fig. 18 illustrates the

summation of all joint torques for the right hand with the neutral configuration in Table 2.

Fig. 17 Grasping a cylinder

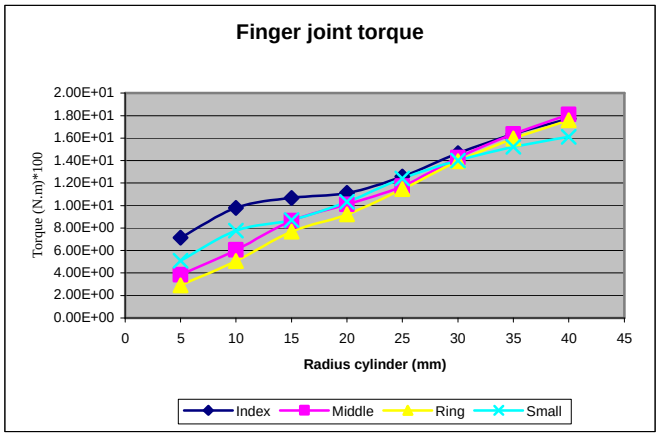


Fig. 18 Finger joint torque

| Neutral gesture of the right hand | | | | |
|---|---|---|---|---|
| Thumb | Index | Middle | Ring | Little |
| $q_1$ =0 | $q_6$ =0 | $q_{10}$ =0 | $q_{14}$ =0 | $q_{20}$ =0 |
| $q_2$ =0 | $q_7$ =30 | $q_{11}$ =30 | $q_{15}$ =2 | $q_{21}$ =5 |
| $q_3$ =30 | $q_8$ =30 | $q_{12}$ =30 | $q_{16}$ =0 | $q_{22}$ =0 |
| $q_4$ =0 | $q_9$ =10 | $q_{13}$ =10 | $q_{17}$ =30 | $q_{23}$ =30 |
| $q_5$ =30 | | | $q_{18}$ =30 | $q_{24}$ =30 |
| | | | $q_{19}$ =10 | $q_{25}$ =10 |

Table 2 Angles for the neutral gesture of the right hand (in degrees)

Another example to determine the joint torques is shown in Fig. 19. The right hand grasps one object and the contact forces are 2 Newtons at each contact point of the finger segments. The joint torques are shown in Fig. 20.

Fig. 19 Power grasping

The problem that it is given joint torques and to find the finger contact forces is a little bit more complicated because we cannot directly use inverse Jacobian matrices to solve the linear equations. One example is shown in Fig. 21. The virtual human hand grasps the object using prehension grasping. The joint torques are given in Fig. 22.

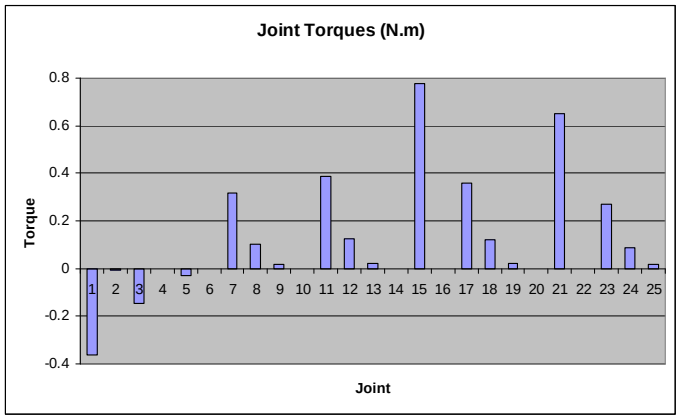


Fig. 20 Finger joint torque

Fig. 21 Finger joint torque

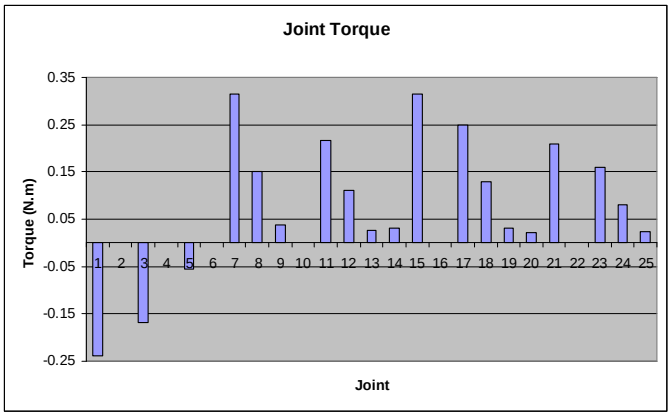


Fig. 22 Given joint torques

The calculated finger contact forces are 3.5N, 4.0N, 2.5N, 3.0N, and 2.5N for the thumb, index, middle, ring and the pinky fingers, respectively.

## CONCLUSION

In this paper, we have introduced methods for posture prediction and force/torque analysis of human hands. A closed-form approach is presented for finger's reach envelope, an optimization-based inverse kinematic method for hand posture prediction, and a systematic method has been proposed to determine the finger contact forces/joint torques. Examples are used to demonstrate the methods. Posture prediction of the human hand will be validated using motion capture system and the joint toque/force will be validate by experimental approach in the near future.

## ACKNOWLEDGMENTS

This research was partly funded by the US Army TACOM project: Digital Humans and Virtual Reality for Future Combat Systems (FCS) and Caterpillar project: Digital Human Modeling and Simulation for Safety and Serviceability.

## REFERENCES

1. Beck, D.J. and Chaffin, D.B., 1992, "An evaluation of inverse kinematics models for posture prediction", *Computer Applications in Ergonomics, Occupational Safety and Health*, Elsevier, Amsterdam, pp. 329-336.
2. B. Buchcholz, T.J. Armstrong & S.A. Goldstein, *Anthropometric data for describing the kinematics of the human hand*, Ergonomics, 35(3), 1992,261-273.
3. Das, B. and Behara, D.N., 1998, "Three-dimensional workspace for industrial workstations", *Human Factors*, Vol. 40, No. 4, pp. 633-646.
4. Denavit, J. and Hartenberg, R.S., 1955. A Kinematic Notation for Lower-Pair Mechanisms Based on Matrices, *Journal of Applied Mechanics*, vol.77, 215-221.
5. Dysart, M. J., and Woldstad, J. C., 1996. Posture prediction for static sagittal-plane lifting. *Journal of Biomechanics*, 29(10), 1393-1397.
6. Faraway, J.J., Zhang, X.D. and Chaffin, D.B., 1999, "Rectifying postures reconstructed from joint angles to meet constraints", *Journal of Biomechanics*, Vol. 32, pp. 733-736.
7. Gill, P., Murray, W., and Saunders, A, 2002, SNOPT: An SQP Algorithm for Large-Scale Constrained Optimization, *SIAM Journal of Optimization*, Vol. 12, No. 4, 979-1006.
8. Jung, E. S., Choe, J., and Kim, S-H., 1994, Psychophysical cost function of joint movement for arm reach posture prediction. *Proceedings of the 38th Annual Meeting of the Human Factors and Ergonomics Society,* 1(1-2), 636-640.
9. Jung, E. S., and Kee, D., 1996. A man-machine interface model with improved visibility and reach functions. *Computers & Industrial Engineering*, 30 (3), 475-486.
10. Jung, E. S., and Choe, J., 1996. Human reach posture prediction based on psychophysical discomfort. *International Journal of Industrial Ergonomics*, 18 (2-3), 173-179.
11. Jung, E.S., and Kang, D., 1995. An object-oriented anthropometric database for developing a man model. *International Journal Of Industrial Ergonomics*, 15(2), 103-110
12. Jung, E S., Chung, M K., Upper Body Reach Posture Prediction for Ergonomics Evaluation Models, *International Journal of Industrial Ergonomics*, v16 n2 1995, 95.
13. Jung, E S.; Kee, D; Chung, M K., Reach posture prediction of upper limb for ergonomic workspace evaluation, *Proc. 36th Annual Meeting of the Human Factors Society*, Part 1 (of 2) Oct 12-16 1992 v 1, Atlanta, GA, 702-706.
14. Kee, D., Jung, E. S., and Chang, S., 1994. A man-machine interface model for ergonomic design. *Computers & Industrial Engineering*, 27 (1-4), 365-368.
15. Kee, D., and Kim, S-H., 1997. Analytic generation of workspace using the robot kinematics. *Computers & Industrial Engineering*, 33(3,4), 525-528.
16. Lee, S.W., and Zhang, X., Development and evaluation of an optimization-based model for power-grip posture prediction, Journal of Biomechanics, 38 (2005), 1591-1597.
17. Pena Pitarch, E., Yang, J., and Abdel-Malek, Santos™ Hand: A 25 Degree-of-Freedom Model, SAE Technical Paper 2005-01-2727.
18. Wang, X, 1999, Behavior-based inverse kinematics algorithm to predict arm prehension postures for computer-aided ergonomic evaluation, *Journal of Biomechanics*, 32(5), 453-460.
19. Yang, J., Abdel-Malek, K., and Nebel, K., "On the Determination of Driver Reach and Barriers," *International Journal of Vehicle Design*, Vol. 37, No. 4, 253-273, 2005.
20. Zhang, X. and Chaffin, D.B., 1996, "Task effects on three-dimensional dynamic postures during seated reaching movements: an analysis method and illustration", *Proceedings of the 1996 40th Annual Meeting of the Human Factors and Ergonomics*

*Society*, Philadelphia, PA, Part 1, Vol. 1, pp. 594-598.

## CONTACT

Dr. Jingzhou Yang, Virtual Soldier Research (VSR) Program, Center for Computer Aided Design, The University of Iowa, Iowa City, IA 52242, Tel: 319-353-2249, Fax: 319-384-0542, E-Mail: jyang@engineering.uiowa.edu.